Orbital Polaron Lattice Formation in Lightly Doped $La_{1-x}Sr_xMnO_3$

J. Geck,[1,2] P. Wochner,[2] S. Kiele,[1,3] R. Klingeler,[1] P. Reutler,[1,4] A. Revcolevschi,[4] and B. Büchner[1]

[1]*Leibniz Institute for Solid State and Materials Research IFW Dresden, Helmholtzstr. 20, 01069 Dresden, Germany*
[2]*Max-Planck-Institut für Metallforschung, Heisenberg Str. 3, 70569 Stuttgart, Germany*
[3]*Hamburger Synchrotronstrahlungslabor HASYLAB at Deutsches Elektronen-Synchrotron DESY, Notkestr. 85, 22603 Hamburg, Germany*
[4]*Laboratoire de Physico-Chimie de l'Etat Solide, Université de Paris-Sud, 91405 Orsay Cedex, France*

(Received 4 November 2004; published 29 November 2005)

By resonant x-ray scattering at the Mn K edge on $La_{7/8}Sr_{1/8}MnO_3$, we show that an orbital polaron lattice (OPL) develops at the metal-insulator transition of this compound. This orbital reordering explains consistently the unexpected coexistence of ferromagnetic and insulating properties at low temperatures, the quadrupling of the lattice structure parallel to the MnO_2 planes, and the observed polarization and azimuthal dependencies. The OPL is a clear manifestation of strong orbital-hole interactions, which play a crucial role for the colossal magnetoresistance effect and the doped manganites in general.

DOI: 10.1103/PhysRevLett.95.236401 PACS numbers: 71.30.+h, 61.10.Eq, 64.60.Cn, 71.27.+a

During the last 20 years there have been tremendous efforts worldwide to unravel the physics behind the doping induced changes in magnetic transition metal oxides. Besides the high-temperature superconducting copper oxides, where the interplay of spins and charges is relevant [1], the physics of doped manganites has become another main focus in this field. In these materials not only are the spins and the charges important, but also the so-called orbital degree of freedom plays a central role for the physical properties [2]. This is already documented by the insulating ground state of undoped $LaMnO_3$, which does not only display antiferromagnetic (AFM) order but also antiferro-orbital order, meaning that the spatial distribution of the $3d$ electrons alternates from one Mn site to the next [3]. Doping of this correlated magnet with holes results in a large number of intriguing physical phenomena. The most prominent is the colossal magnetoresistance (CMR) effect, i.e., the enormous suppression of the electrical resistivity in applied magnetic fields.

On a qualitative level, the CMR can be understood in terms of the double exchange (DE) model. The DE mechanism refers to spin-charge interactions only and implies that parallel spin alignment and charge itineracy are equivalent. Nonetheless, bare spin-charge scenarios fail to describe the CMR effect on a quantitative level [4]. An even more clear example for the failure of bare spin-charge scenarios is the ferromagnetic insulating (FMI) phase of lightly doped $La_{1-x}Sr_xMnO_3$ around the commensurate doping level $x = 1/8$. The apparent contradiction between the FMI properties and the DE clearly indicates that the other degrees of freedom referring to the lattice and the orbitals are indispensable to understand the physics of the manganite materials. In the case of the FMI phase, this conjecture agrees with the observed complex structural modulations that point to a complex ordering of lattice and orbital degrees of freedom [5–9].

Indeed, in a previous publication we could show that the development of the FMI phase of $La_{7/8}Sr_{1/8}MnO_3$ below the metal-insulator transition at T_{MI} is connected to an orbital reordering [10]. But despite extensive theoretical and experimental effort, there is no consensus about the type of ordering, as manifested by the large variety of different models proposed in the literature [6–8,11–13]. In order to clarify the microscopic nature of the FMI phase and to identify the relevant interactions, we have performed resonant x-ray scattering (RXS) experiments at the Mn K edge on $La_{7/8}Sr_{1/8}MnO_3$. Obviously, to be able to observe the complex orbital arrangement of only one electron per Mn^{3+} site, ordinary diffraction is not sufficient. By using in addition the spectroscopic signature of the Mn^{3+} valence orbitals, appropriate positions in reciprocal space as well as the dependence of the scattering intensity on the mutual orientation of x-ray polarization vector and orbital orientation, we achieve enough sensitivity in this ''spectro-diffraction'' that we can unambiguously determine the long-range ordered orbital configuration.

The experimental data provide firm experimental evidence for the formation of an orbital polaron lattice (OPL) at low temperatures, which unifies ferromagnetic and insulating properties in a natural way. To our knowledge, the OPL is the first microscopic model reproducing the correct unit cell. Furthermore, the OPL in the FMI phase constitutes a clear manifestation of strong orbital-hole interactions, which play a crucial role for the doping induced transition from an AFM insulating to a FM metallic state and are of crucial importance for the physics of doped manganites in general.

In the course of the present RXS study, two $La_{7/8}Sr_{1/8}MnO_3$ single crystals with carefully polished (001) and (112) surfaces have been investigated (*Pbnm* setting). The samples have been prepared from the same sample rod, obtained by the traveling floating zone method [14]. Although there are six possible structural twin domains, whose [100], [010], and ⟨112⟩ directions can coincide, in our samples only a subset of twins is realized, where [100] or [010] directions (type A twins) never over-

lap with ⟨112⟩ directions (type B twins) [10]. Further experimental details about the RXS experiment, which has been performed at the wiggler beam line W1 at HASYLAB, can be found in the literature [10].

Upon cooling the samples from room temperature to 10 K, in addition to a symmetry change from orthorhombic to monoclinic and triclinic, several types of structural modulations have been observed. The corresponding superstructure reflections can be grouped into (I) so-called ATS reflections, (II) reflections with modulation wave vector $(0, 0, 1/2)$, (III) reflections with $(1/4, -1/4, 0)$, and (IV) reflections with $(1/2, 1/2, 0)$. The ATS (anisotropy of the tensor of susceptibility) reflections of (I) are forbidden reflections due to glide plane and screw axis symmetries, e.g., (300), (030), (003), or (104), which can be observed in resonance at the Mn K edge [15]. The reflections belonging to the groups (II)–(IV) appear only in the FMI phase below $T_{\mathrm{MI}} \simeq 150$ K. Group (II) reflections have been discussed in terms of charge order [8–10] and group (IV) reflections in terms of an orbital rearrangement [10].

The studies on the (112)-oriented sample proved the occurrence of a superstructure reflection at the nominal $(1.75, 2.25, 4)$ position in the FMI phase (group III). Since there is no superposition of type A and type B twins in our samples, the observation of the nominal $(1.75, 2.25, 4)$ reflection unambiguously shows that a quadrupling along the orthorhombic $[1\bar{1}0]$ or $[110]$ exists below T_{MI}. The energy dependence of the intensity at the $(1.75, 2.25, 4)$ position displays a diplike feature around the Mn K edge, as can be observed in Fig. 1(a). This implies a dominant contribution to the intensity due to the heavy nonresonant scatterers, which participate in the corresponding superstructure modulation [Fig. 1(b)]. Note that this type of energy dependence does not allow one to infer anything about possible charge and/or orbital order, as has been done in the literature [11]. Even in the naïve case of ordered Mn^{3+} and Mn^{4+} ions, the corresponding resonance can be easily masked by the signal of the heavier nonresonant sites.

To summarize so far, the present RXS measurements reveal a superstructure modulation in the FMI phase, which involves a doubling along the c direction and a quadrupling parallel $[1\bar{1}0]$ or $[110]$. Furthermore, the $(3/2, 3/2, 3)$ reflection (group IV) signals a doubling along $[1\bar{1}0]$ or $[110]$. The twinning prevents a unique identification, but because the $(1.75, 2.25, 4)$ reflection displays a dip at the Mn K edge, while a resonance is observed at the $(3/2, 3/2, 3)$ position [cf. Ref. [10]], it is tempting to assign them mutual orthogonal directions. This result is in agreement with a selected area electron diffraction (SAED) study which probes a single twin domain [5]. Both the RXS and the SAED data imply a $2a_c \times 4b_c \times 4c_c$ unit cell in the FMI phase, where the subscript c indicates the pseudocubic lattice parameters of the high-temperature orthorhombic phase (cf. Fig. 2). To the best of our knowledge, the quadrupling along the pseudocubic b direction is not

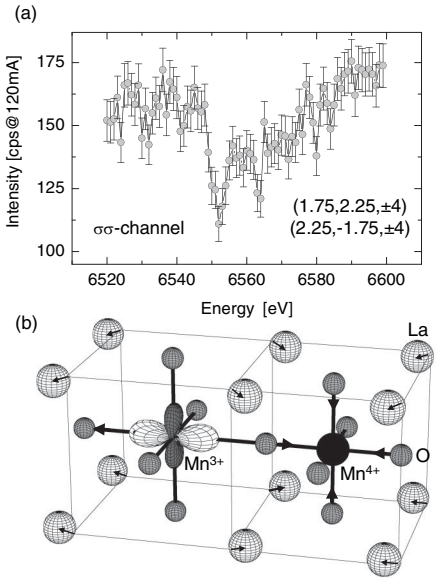

FIG. 1. (a) Energy dependence of the intensity at the nominal $(1.75, 2.25, 4)$ position taken at $T = 50$ K (without absorption corrections). (b) Illustration of a distortion that involves the heavy La sites. The gray and white lobe represents the spatial e_g-electron distribution of a Mn^{3+} site that corresponds to about $1/100$ of the total charge per unit cell. The breathing distortion at the Mn^{4+} site and shifts of the La sites are indicated by arrows.

reproduced by any of the published microscopic models for the FMI phase of $La_{7/8}Sr_{1/8}MnO_3$ [6–9,11–13], which calls for the development of a model based on the correct unit cell. In a first approximation we will assume a strong localization of the doped holes, which is well verified by the pronounced insulating properties of the FMI phase [16]. Furthermore, we will omit the small triclinic distortion present below T_{MI} [17].

The superstructure modulation signaled by reflections of the type $(h, k, l + 0.5)$, which are observed in neutron and x-ray scattering experiments, as well as Hartree-Fock and LSDA + U calculations, provide strong evidence for an alternation of hole-rich and hole-poor planes along the orthorhombic c direction below T_{MI} [6,8,9,12,13]. The terms hole-poor and hole-rich indicate that there is not necessarily a perfect segregation into completely undoped and doped planes. Similarly, the terms hole-poor and hole-rich Mn sites will be used to stress that the valence difference δq between $Mn^{3.5+\delta q}$ and $Mn^{3.5-\delta q}$ can be less than $\delta q = 0.5$. The theoretical model calculations also yield an antiferro-orbital ordering within the hole-poor planes [12,13], indicating that the superexchange and/or electron-lattice interactions which stabilize this type of orbital order [18] are still relevant in the FMI phase. In what follows, these interactions will be represented by the coupling constant J. Hole induced interactions due to lattice distortions as well as Coulomb and double exchange interactions [19,20] will be summarized by the coupling constant Δ, hereafter. The interactions J and Δ both determine the orbital occupation at a given hole-poor, i.e.,

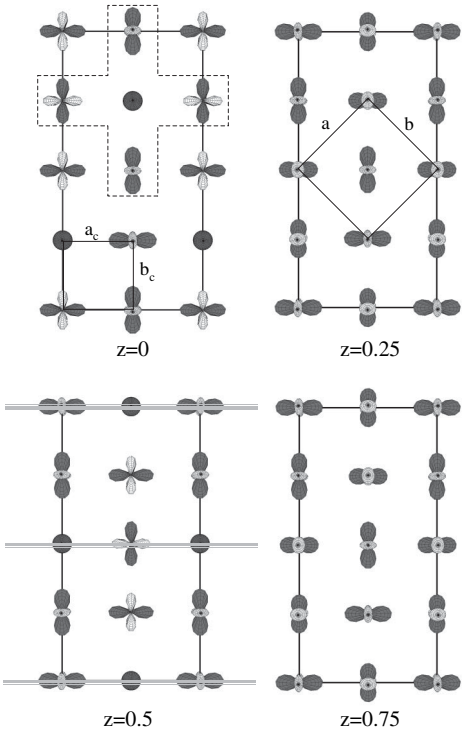

FIG. 2. Orbital polaron model for the FMI phase of $La_{7/8}Sr_{1/8}MnO_3$. A top view of the different *ab* planes along the *c* axis is shown. The orbitals have been calculated according to the interaction $\mathcal{H}_{\mathrm{OP}}$ with $\Delta/J = 1$. The orthorhombic (a, b) as well as the pseudocubic (a_c, b_c) lattice parameters are indicated. The hatched cross ($z = 0$) and the gray bars ($z = 0.5$) mark the orbital polaron and charge stripes in the *ab* planes, respectively.

Mn^{3+}-like site, next to a hole. In terms of a mean field approach, this can be modeled by Hamiltonians of the form $\mathcal{H}_{\mathrm{OP}} = -(J\sigma^x + \Delta\sigma^y)$, which describe these interactions parallel to the *c* direction ($\sigma^{x,y}$: Pauli matrixes) [19]. Based on $\mathcal{H}_{\mathrm{OP}}$, the alternation of hole-poor and hole-rich planes along the *c* direction, and the $2a_c \times 4b_c \times 4c_c$ unit cell, we obtain a model for the FMI phase, which is depicted in Figs. 2 and 3 for $J/\Delta = 1$. The interaction J establishes an almost complete antiferro-orbital order within the hole-poor planes. However, due to the additional orbital-hole interaction Δ the antiferro-orbital ordering is modified. This is most evident in the hole-rich planes ($z = 0, 0.5$) in Fig. 2. Δ induces a polarization of the orbitals next to a hole and, consequently, the model constitutes an OPL.

In order to check whether the ordering represented in Fig. 2 is consistent with our experimental RXS results, we performed a model calculation based on the OPL. The sensitivity to orbital order of RXS at the Mn *K* edge stems from the fact that at this energy the scattering process involves Mn:4*p*-intermediate states. The energy splitting of the Mn:4*p* states reflects the orbital occupation at a given Mn site l and gives rise to a characteristic anisotropy of the corresponding form factor f_l with respect to the beam polarization [3]. This polarization dependence can be described as $f_l(\epsilon_i, \epsilon_f) = \epsilon_f^t \cdot \hat{f}_l \cdot \epsilon_i$, with the second rank tensor $\hat{f}_l$ and the polarization vectors ϵ_i and ϵ_f of the incoming and outgoing beam, respectively. In the following, σ or π polarization refer to polarizations $\perp$ and parallel to the scattering plane, respectively [cf. [10]]. For the hole-poor sites we take the $\hat{f}_l$ to be diagonal with diagonal elements $f_l^{\alpha,\alpha} = f^{\mathrm{hp}}(1 + \delta_l^\alpha)$ $(\alpha = x, y, z)$, where the $\delta_l^{x,y,z}$ are related to the splitting of the Mn:4*p* states. As a result, the symmetry of the tensors $\hat{f}_l$ corresponds to the symmetry of the orbitals in Fig. 3. The hole-rich sites are described by an isotropic $\hat{f}_l$, i.e., $f_l^{\alpha,\alpha} = f^{\mathrm{hr}}$. Using the set of basis sites shown in Fig. 3 and the form factors described above, the structure factor matrix for a reflection Q can be calculated: $\hat{F}(Q) = \sum_l \hat{f}_l \cdot e^{id_l \cdot Q}$, where d_l describes the position of lattice site l. The resonantly scattered intensity $I(Q) = |\epsilon_f^t . \hat{F}(Q) . \epsilon_i|^2$ is polarization dependent and displays a characteristic variation, when the sample is rotated about ψ around the scattering vector Q. This is the so-called azimuthal dependence. A straightforward calculation yields the following expressions for the azimuthal dependencies of the (1.5 1.5 3) reflection:

$$I_{\sigma\pi} = A\sin^2\vartheta\cos^2\psi\sin^2\psi + B\cos^2\vartheta\sin^2\psi$$

$$I_{\sigma\sigma} = A'\sin^4\psi + \text{const.}$$

For the (300) reflection $I_{\sigma\pi} = A''\cos^2\vartheta\sin^2\psi$ and $I_{\sigma\sigma} = 0 + \mathcal{O}(\delta^2)$ is obtained. In the above equations, ϑ is the scattering angle; the constants A, A', A'', and B are functions of the matrix elements of the $\hat{f}_l$. In addition, the indices σ and π refer to the initial and final beam polarization (see Fig. 4). The matrix elements have been used as

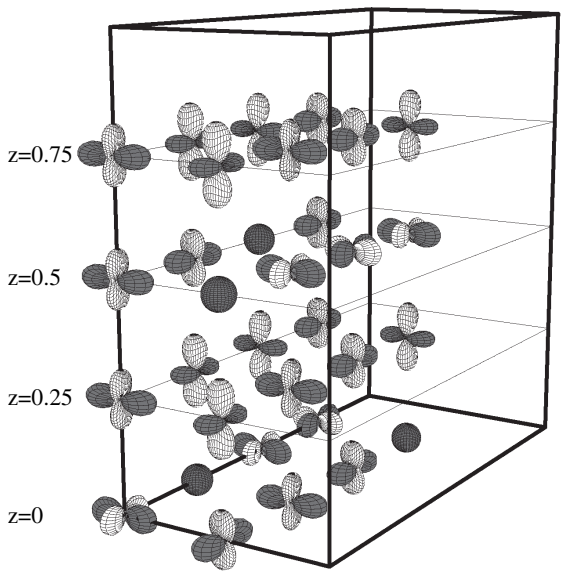

FIG. 3. Basis of the orbital polaron model for the FMI phase of $La_{7/8}Sr_{1/8}MnO_3$ which has been used for the calculation of the structure factor. The thick solid lines indicate the $2a_c \times 4b_c \times 4c_c$ supercell.

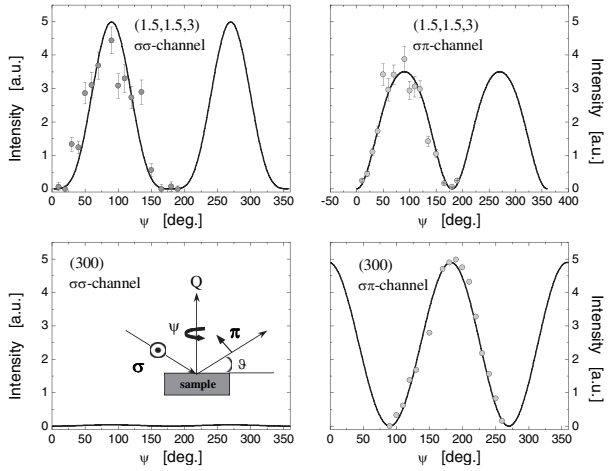

FIG. 4. Comparison between the measured data and a model calculation based on the orbital polaron lattice. The model calculation, which takes into account the twinning of the sample, reproduces the polarization dependencies observed at the nominal (300) and (1.5, 1.5, 3). A $\sigma\pi$-scattering process is sketched in the lower left panel.

parameters to fit the azimuthal dependencies of the (300) and the (1.5 1.5 3) simultaneously. As demonstrated in Fig. 4, the OPL model nicely reproduces the polarization dependencies observed at the nominal (300) and (1.5 1.5 3) position. In particular, the model is capable of reproducing the relative intensities observed at the (300) and the (1.5 1.5 3) position in the $\sigma\sigma$ and the $\sigma\pi$ channel, although it has to be noted that the fitted components of the $\hat{f}_i$ could not be determined unambiguously. But we emphasize that the simultaneous description of the data in Fig. 4 provides very strict constraints for the orbital polaron order. For example, an OPL based on the charge ordering pattern proposed in Ref. [6] always leads to $I_{\sigma\sigma} = \mathcal{O}(\delta)$ for the (300) reflection; i.e., there is always a significant intensity in the $\sigma\sigma$ channel. The ordering shown in Fig. 2 is similar to one of the ground states obtained by Hartree-Fock calculations for $La_{7/8}Sr_{1/8}MnO_3$ [12], supporting the scenario developed above. Note that orbital polarons are ferromagnetic objects which lead to a strong reduction of the charge carrier bandwidth [19]. A closer look at the OPL shows that there is always a nonvanishing overlap between an empty and an occupied e_g state; i.e., the resulting exchange interactions are all ferromagnetic. As a result, the OPL unifies ferromagnetic and insulating properties. Interestingly, according to this model half doped charge stripes exist below T_{MI}. Since these stripes run along the a_c direction, which is doubled below T_{MI}, one may speculate whether a mechanism similar to a Peierls effect is relevant for the FMI phase.

It is important to note that there is clear experimental evidence that local charge hopping (DE) processes contribute significantly to the stabilization of the FMI phase [21,22]. This is in perfect agreement with the OPL model, because orbital polarons are stabilized by local DE processes. Furthermore, the phase diagram of $La_{1-x}Sr_xMnO_3$ as a function of x can be reproduced by a model where the OPL formation competes with the AF-orbital order and with orbital fluctuations [19]. This competition together with the importance of local DE processes also explains the stability of the OPL in other compounds. For instance, in lightly doped $La_{1-x}Ca_xMnO_3$ and $Pr_{1-x}Ca_xMnO_3$ the DE interaction is reduced and, correspondingly, the AF-orbital ordering is observed instead of the OPL [23,24]. Nonetheless, the tendency to form orbital polarons is also expected to be present in these systems. We emphasize that the OPL has been derived based on the interactions described by $\mathcal{H}_{\mathrm{OP}}$, which means that the OPL is a direct manifestation of strong orbital-hole interactions in doped manganites. Furthermore, it can be concluded that these interactions are strongly spin dependent, since the DE mechanism is found to contribute significantly to the stabilization of the FMI phase [22]. According to the above discussion, the spin-dependent orbital-hole interaction is a general feature of doped manganite compounds and it is clear that such an interaction is of great relevance for the CMR effect.

We are very grateful to H. Dosch for his support. Furthermore, the authors would like to thank M. v. Zimmermann for fruitful discussions.

[1] J. Orenstein and A. J. Millis, Science **288**, 468 (2000).
[2] Y. Tokura and N. Nagaosa, Science **288**, 462 (2000).
[3] Y. Murakami *et al.*, Phys. Rev. Lett. **81**, 582 (1998).
[4] A. J. Millis *et al.*, Phys. Rev. Lett. **77**, 175 (1996).
[5] K. Tsuda *et al.*, J. Phys. Soc. Jpn. **70**, 1010 (2001).
[6] Y. Yamada *et al.*, Phys. Rev. Lett. **77**, 904 (1996).
[7] T. Inami *et al.*, Jpn. J. Appl. Phys., Suppl. **38-1**, 212 (1999).
[8] Y. Yamada *et al.*, Phys. Rev. B **62**, 11 600 (2000).
[9] T. Niemoeller *et al.*, Eur. Phys. J. B **8**, 5 (1999).
[10] J. Geck *et al.*, Phys. Rev. B **69**, 104413 (2004).
[11] Y. Endoh *et al.*, Phys. Rev. Lett. **82**, 4328 (1999).
[12] T. Mizokawa *et al.*, Phys. Rev. B **61**, R3776 (2000).
[13] M. Korotin *et al.*, Phys. Rev. B **62**, 5696 (2000).
[14] P. Reutler *et al.*, J. Cryst. Growth **249**, 222 (2003).
[15] V. E. Dmitrienko, Acta Crystallogr. Sect. A **39**, 29 (1983).
[16] S. Uhlenbruck *et al.*, Phys. Lett. **82**, 185 (1999).
[17] D. E. Cox *et al.*, Phys. Rev. B **64**, 024431 (2001).
[18] L. F. Feiner *et al.*, Phys. Rev. B **59**, 3295 (1999).
[19] R. Kilian *et al.*, Phys. Rev. B **60**, 13 458 (1999).
[20] J. Bała *et al.*, Phys. Rev. B **65**, 134420 (2002).
[21] J. Geck *et al.*, New J. Phys. **6**, 152 (2004).
[22] R. Klingeler *et al.*, Phys. Rev. B **65**, 174404 (2002).
[23] M. v. Zimmermann *et al.*, Phys. Rev. B **64**, 195133 (2001).
[24] Z. Jirak *et al.*, J. Magn. Magn. Mater. **53**, 153 (1985).